Energy Spectra for Decaying 2D Turbulence in a Bounded Domain

H. J. H. Clercx and G. J. F. van Heijst

Department of Physics, Eindhoven University of Technology, P.O. Box 513, 5600 MB Eindhoven, The Netherlands

(Received 14 September 1999; revised manuscript received 27 March 2000)

New results are presented for the energy spectra of decaying 2D turbulence in a square container with no-slip walls for integral-scale Reynolds numbers up to 20 000. The one-dimensional energy spectra measured close to the walls reveal a $k^{-5/3}$ inertial range, instead of a k^{-3} direct enstrophy cascade, due to the production of small-scale vorticity near no-slip boundaries. During the intermediate decay stage a k^{-3} spectrum starts to emerge and the change in location of the injection scale of small-scale vorticity is explained in terms of an average boundary-layer thickness.

PACS numbers: 47.27.Eq, 47.27.Ak

Thirty years ago the first phenomenological theory of two-dimensional (2D) turbulence was presented by Kraichnan [1] and by Batchelor [2]. Following this theory, the energy spectrum shows an inverse energy cascade (the $k^{-5/3}$ spectrum) for $k < k_i$, with k_i the wave number associated with the injection scale of the forcing, and a direct enstrophy cascade (the k^{-3} spectrum) for $k > k_i$. Since these pioneering theoretical studies many numerical investigations have been carried out in order to find supporting evidence for the presence of an inverse energy cascade and a direct enstrophy cascade, and the associated inertial range spectra, in 2D turbulence [3–8]. For the same reasons several experimental investigations have been carried out [9–12].

Numerical studies of forced 2D turbulence with periodic boundary conditions more or less support the Kraichnan-Batchelor picture [3,7,8], although Legras *et al.* [7] observed steeper spectra for large wave numbers (small scales). Numerical simulations of decaying 2D turbulence with periodic boundary conditions show a more intricate behavior of the energy spectra: the inverse energy cascade is usually not very clearly observed and the direct enstrophy cascade is often established only as a transient state before the viscous range starts to dominate [4,5]. Additionally, the appearance of coherent vortices complicates a comparison of the spectra of decaying 2D turbulence with the Kraichnan-Batchelor theory. It is assumed that due to the presence of a hierarchy of coherent vortices the energy spectrum becomes more steep [4]. Experiments [9–12] to confirm the presence of the inverse energy cascade, the direct enstrophy cascade, or both cascades simultaneously are even more complicated. This is due to the restriction to flows with intermediate or low integral-scale Reynolds number ($\mathrm{Re} \leq 2000$) in 2D turbulence experiments in thin, magnetically forced, fluid layers [9,10], or due to the lack of 2D incompressibility in soap film experiments which is a consequence of thickness fluctuations [11,12] (note that in the latter experiments higher integral-scale Reynolds numbers can be achieved). Despite the complications associated with soap film experiments, Kellay *et al.* [11] were able to show evidence for the presence of a direct enstrophy cascade in decaying 2D turbulence by means of homodyne photon correlation spectroscopy and by optical fiber velocimetry. Recently, Rutgers [12] measured the simultaneous presence of the $k^{-5/3}$ and the k^{-3} spectrum in forced 2D turbulence using laser Doppler velocimetry. All experimental setups mentioned above disregard the role of (no-slip) boundaries. Moreover, the arrangement of the experiments to measure the spectrum is often not suitable to obtain 1D spectra close to boundaries.

In this Letter we report new results of energy spectra for decaying 2D turbulent flows in a square container with no-slip walls. The numerical simulations of the 2D Navier-Stokes equations on a bounded domain were performed with a 2D dealiased Chebyshev pseudospectral method, with a maximum of 513 Chebyshev modes in each direction for $\mathrm{Re} = 20\,000$ (361 modes for $\mathrm{Re} = 10\,000$ and 257 modes for $\mathrm{Re} = 5000$). The numerical computations of decaying 2D Navier-Stokes turbulence with periodic boundary conditions were carried out with a standard 2D Fourier pseudospectral method with a maximum of 341 active Fourier modes in each direction. In both cases neither hyperviscosity nor any other artificial dissipation has been used. The integral-scale Reynolds number of the flow is defined as $\mathrm{Re} = UW/\nu$ with U the rms velocity of the initial flow field, W the half-width of the container, and ν the kinematic viscosity of the fluid. Time has been made dimensionless by W/U and vorticity by U/W. The initial microscale Reynolds number is defined as $\mathrm{Re}_{\mathrm{micr}} = 2\,\mathrm{Re}/\omega_0$, with ω_0 the (dimensionless) initial rms vorticity. In our numerical experiments $\omega_0 = 38.0 \pm 0.5$, thus corresponding with $\mathrm{Re}_{\mathrm{micr}} \cong 263$, 526, and 1052, respectively. The time τ is defined as $\tau = \frac{\omega_0 t}{N}$, with t the dimensionless time and N^2 the number of vortices present in the initial flow field, and $\tau = 1$ corresponds approximately with the (initial) eddy turnover time.

The initial condition for the velocity field consists of 100 nearly equal-sized Gaussian vortices (thus $N = 10$). The vortices have a dimensionless radius of 0.05 and a dimensionless absolute vortex amplitude $|\omega_{\max}| \cong 100$. Half of the vortices have positive circulation, and the other vortices have negative circulation. The vortices are placed on a regular lattice, initially well away from the boundaries,

 0031-9007/00/85(2)/306(4)$15.00

with a random displacement of the vortex centers equal to approximately 6% of the dimensionless lattice parameter λ, with $\lambda \cong 0.17$. A smoothing function, similar to the one employed in Ref. [13], has been used in order to ensure the no-slip condition exactly. The initial conditions for the simulations with periodic boundary conditions are the same.

The spectra discussed in this Letter are computed from an ensemble average of 12 runs for Re = 5000, an ensemble average of 8 runs for Re = 10 000, and from an average of 2 runs for the simulations with Re = 20 000.

Figure 1 shows some snapshots of the vorticity distribution of decaying turbulence for Re = 20 000 in a container with no-slip boundaries (Figs. 1a and 1b) and for the case with periodic boundary conditions (Figs. 1c and 1d). It can be concluded that already at early times in the flow evolution strong vortex-wall interactions can be observed and that huge amounts of small-scale vorticity are produced near the no-slip walls.

A geometry with walls is no longer well approximated as isotropic and homogeneous in nature and so the dimensional arguments leading to the $k^{-5/3}$ and k^{-3} slope lose their validity and such spectra are not expected *a priori*. One of the tools to understand the role of the boundaries on the evolution of turbulence is by comparing the energy

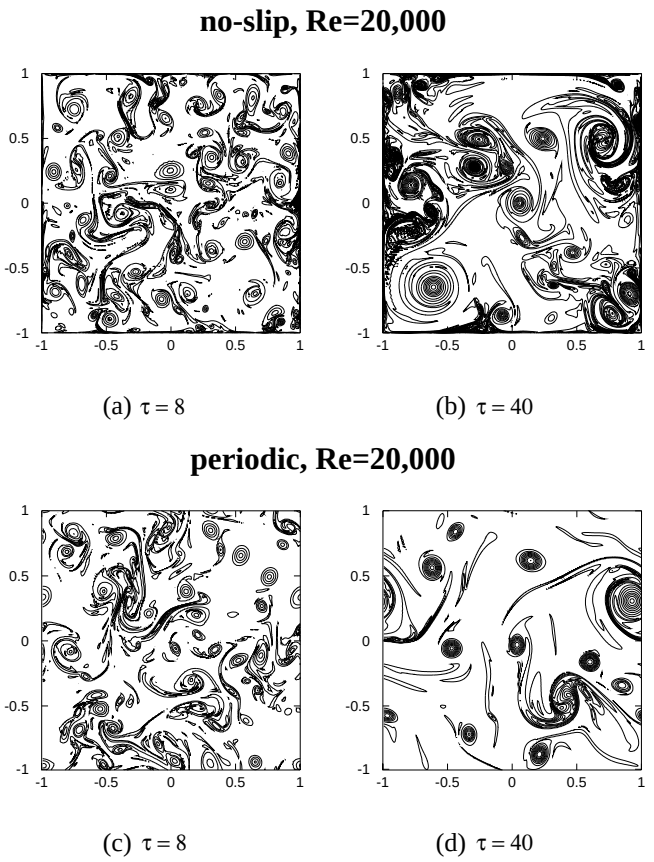

FIG. 1. Vorticity contour plots of the simulations with no-slip (a),(b) and with periodic (c),(d) boundary conditions. The contour level increment in units of ω_0 is (a) and (c) 0.5, (b) and (d) 0.125.

spectra of the no-slip and the periodic cases. Essential for this comparison is the use of an alternative approach to measure the energy spectra. A straightforward procedure is the computation of one-dimensional spectra. A 1D spectrum is obtained by considering the kinetic energy of the flow

$$E(x, y, \tau) = \sum_{n=0}^{N} \sum_{m=0}^{N} \hat{E}_{nm}(\tau) T_n(x) T_m(y), \qquad (1)$$

along the line $x = x_i$ or along the line $y = y_i$. The $T_n(x)$, with $0 \le n \le N$, are the Chebyshev polynomials of order n, the $T_m(y)$ are defined analogously, and the $\hat{E}_{nm}(\tau)$ represent the Chebyshev spectral coefficients of the kinetic energy. The 1D spectrum $\hat{S}_n(\tau)$ is defined as an average of the symmetrically equivalent contributions along the lines $x = a$, $x = -a$, $y = a$, and $y = -a$. The 1D spectrum of the contribution along the line $x = a$, denoted by $\hat{S}_{x=a,n}(\tau)$, is expressed as

$$\hat{S}_{x=a,n}(\tau) = \left| \sum_{m=0}^{N} \hat{E}_{mn}(\tau) T_m(a) \right|_{\Delta\tau}, \qquad (2)$$

where the subscript $\Delta\tau$ states that the 1D spectrum is averaged over the time interval $[\tau - \Delta\tau, \tau]$ (for present results we always used $\Delta\tau = 2$). The 1D spectrum has thus the following form: $\hat{S}_n(\tau) = \frac{1}{4}[\hat{S}_{x=a,n}(\tau) + \hat{S}_{x=-a,n}(\tau) + \hat{S}_{y=a,n}(\tau) + \hat{S}_{y=-a,n}(\tau)]$. The 1D spectra for the simulations with periodic boundary conditions are computed in a similar way.

In Fig. 2a we have plotted the ensemble average of $\hat{S}_n(\tau)$ for Re = 10 000 at $\tau \cong 2$. Both the runs with no-slip and the runs with periodic boundary conditions show a k^{-3} spectrum. Note that a k^{-n} Fourier spectrum results in the same power law Chebyshev spectrum; a direct comparison of Fourier spectra with Chebyshev spectra is thus allowed. From the spectra shown in Fig. 2a it is clear that in a few eddy turnover times, small enough so that the presence of boundaries is negligible yet, the exponential tail of the spectrum, associated with the initial flow field consisting of many Gaussian vortices, is modified into a k^{-3} spectrum. Similar spectra are observed for Re = 5000 and 20 000. In Figs. 2b–2d several averaged spectra for the runs with Re = 20 000 are shown for different locations a and times τ: $a = 0.00$ and $\tau \cong 4$ (Fig. 2b), $a = 0.95$ and $\tau \cong 4$ (Fig. 2c), and finally $a = 0.95$ and $\tau \cong 8$ (Fig. 2d). Each separate plot shows the averaged 1D spectrum for the runs with no-slip (drawn line) and the runs with periodic boundary (dashed line) conditions. A clear $k^{-5/3}$ spectrum can be observed over the complete inertial (see Figs. 2c and 2d) range which strongly deviates from the "classical" spectrum as usually observed for 2D decaying turbulence: the k^{-3} slope, characteristic for the direct enstrophy cascade, is absent. When moving from the boundary to the center of the container we observe a gradual steepening of the spectrum, but it is still considerably less steep than the spectra of the associated runs with periodic boundary conditions.

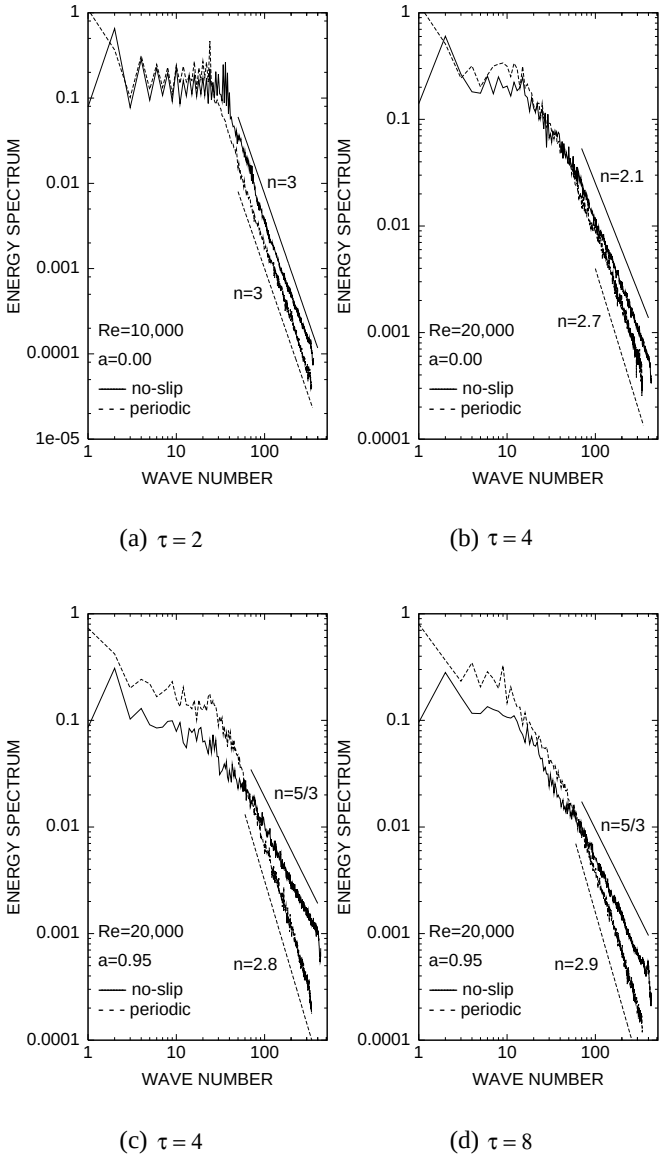

(a) $\tau = 2$ (b) $\tau = 4$

(c) $\tau = 4$ (d) $\tau = 8$

FIG. 2. The 1D energy spectra for runs with no-slip walls and with periodic boundary conditions (the steeper spectrum in the inertial range). The best power law fits for the Chebyshev and the Fourier spectra are represented by the drawn and dashed lines, respectively.

In Figure 3 we have plotted the ensemble averaged 1D spectra, computed near the no-slip boundary ($a = 0.95$), for Re = 5000, 10 000, and 20 000. The inertial range spectra all behave like k^{-n} with $n = 2.4 \pm 0.1$, 1.9 ± 0.1, and 1.7 ± 0.1, respectively. It shows the gradual disappearance of the direct enstrophy cascade when the Reynolds number is increased. From this observation one can conclude that the absence of the direct enstrophy cascade is not a low Reynolds number artifact. On the contrary, the higher the Reynolds number, the more the energy spectrum shows a $k^{-5/3}$ spectrum, underlining the role of the boundaries as a source of small-scale vorticity. The corresponding inertial range spectra for the runs with periodic boundary conditions behave like k^{-n} with $n = 3.1 \pm 0.2$, 3.0 ± 0.2, and 2.8 ± 0.2, respectively, which differs considerably from the confined container case. It should be mentioned that the spectra for the runs with periodic boundary conditions do not behave like pure power laws. The computed power law exponent n is a best estimate; as a consequence slight variations around the value $n = 3$ might be expected. The disappearance of the direct enstrophy cascade near no-slip boundaries has also consequences for the spectra measured at $a = 0$, although not so striking. Estimates of the power law exponents of the ensemble averaged 1D spectra are summarized in Table I. It is clear that the spectra measured in the center of the container with no-slip walls show inertial range spectra with $2.1 \leq n \leq 2.5$, and that a clear direct enstrophy cascade is absent.

The inverse cascade, for $\tau < 10$ observed up to the smallest resolved scales, is actually a consequence of the production of small-scale vorticity at the no-slip boundaries. The injection scale k_i of small-scale vorticity appears to be associated with an average boundary-layer thickness $\delta(\tau)$ which is defined as the ratio between the vorticity and the normal gradient of the vorticity at the boundary. It is expected that $\delta(\tau)$ grows in the course of time. This is supported by the time evolution of the spectra shown for $\tau = 8$, 20, 32, and 120 (from upper to lower curve) in Fig. 4a which shows that for $\tau \geq 20$ the

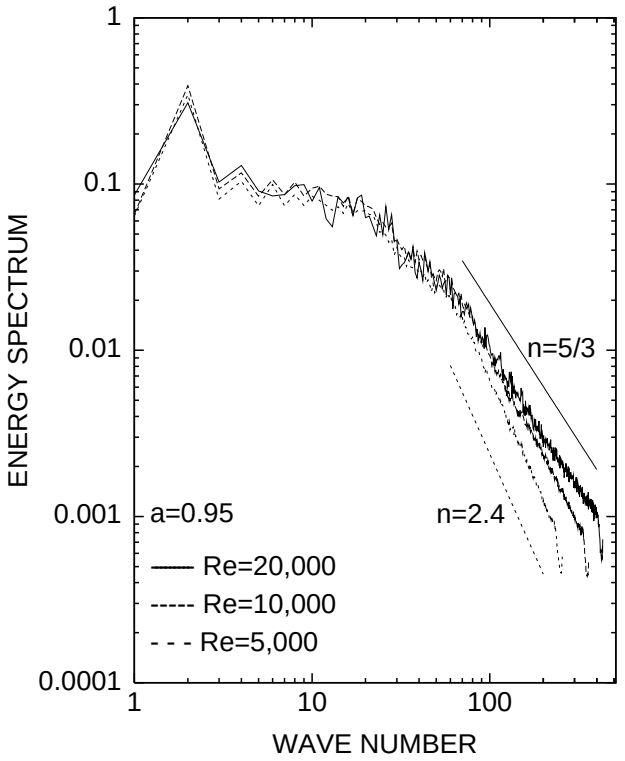

FIG. 3. The 1D energy spectra as function of the wave number for runs with no-slip boundaries. The steepest inertial range spectrum corresponds to the run with Re = 5000 ($n = 2.4$). The inertial range spectrum with $n = 5/3$ corresponds with the Re = 20 000 run. The spectra are measured for $\tau = 4$ and at position $a = 0.95$.

TABLE I. Power law exponents n for runs with no-slip and with periodic boundary conditions for different integral-scale Reynolds numbers. The power law exponents are computed at positions $a = 0.00$ and $a = 0.95$ for $\tau = 4$ and $\tau = 8$.

Re	τ	a	$n_{\text{no-slip}}$	n_{periodic}
20 000	4	0.95	1.7	2.8
		0.00	2.1	2.7
	8	0.95	1.8	2.9
		0.00	2.2	3.0
10 000	4	0.95	1.9	3.0
		0.00	2.4	3.0
	8	0.95	1.9	3.0
		0.00	2.5	3.0
5000	4	0.95	2.4	3.1
		0.00	2.5	2.9
	8	0.95	2.5	2.8
		0.00	2.5	3.0

high wave number part of the $k^{-5/3}$ spectrum slowly transforms into a k^{-3} spectrum, i.e., the injection scale k_i moves to smaller wave numbers (or, equivalently, $\lambda_i \propto k_i^{-1}$ becomes larger) when the average boundary-layer thickness increases. Note that all spectra shown in Fig. 4a reveal a clear $k^{-5/3}$ slope for $k < k_i$. The strong correlation between the wavelength λ_i corresponding to the location of the kink in the spectrum and the average boundary-layer thickness is obvious from the data shown in Fig. 4b. Actually, the following relation is found: $\lambda_i(\tau) \approx 2\delta(\tau)$ (for clearness we did not plot the data on top of each other). The data displayed in Fig. 4b for Re = 20 000 is much more spiky than for Re = 10 000 and 5000 because only two runs were available for averaging. Note that for $\tau < 20$ it is very difficult to observe a kink in the spectrum: for $\tau < 10$ no kink is observed at all and for $\tau \geq 10$ the $k^{-5/3}$ slope tends to become slightly steeper for large wave numbers. From $\tau \approx 20$ the position of the kink can be determined with reasonable accuracy.

In conclusion, we have shown the absence of the direct enstrophy cascade in 1D spectra computed near no-slip walls during the initial decay stage ($\tau < 20$) of 2D turbulence in a bounded domain for Re $\leq$ 20 000. It is conjectured that the direct enstrophy cascade also disappears during the initial decay stage for simulations with higher initial integral-scale Reynolds numbers. However, numerical confirmation is not possible yet due to the large amount of necessary CPU time on a Cray Y-MP C916 for these high Reynolds number runs in domains with no-slip walls. After approximately 20 initial eddy turnover times the spectrum slowly evolves towards the form known from forced 2D turbulence: a $k^{-5/3}$ slope for $k < k_i$ and a k^{-3} slope for $k > k_i$ with k_i the wave number associated with the average boundary-layer thickness. At this wave number small-scale vorticity is injected into the flow. This observation for the late-time spectrum evolution is nevertheless rather surprising because homogeneity and isotropy, necessary assumptions for the Kraichnan-Batchelor theory of 2D turbulence, are absent for turbulent flows in bounded domains.

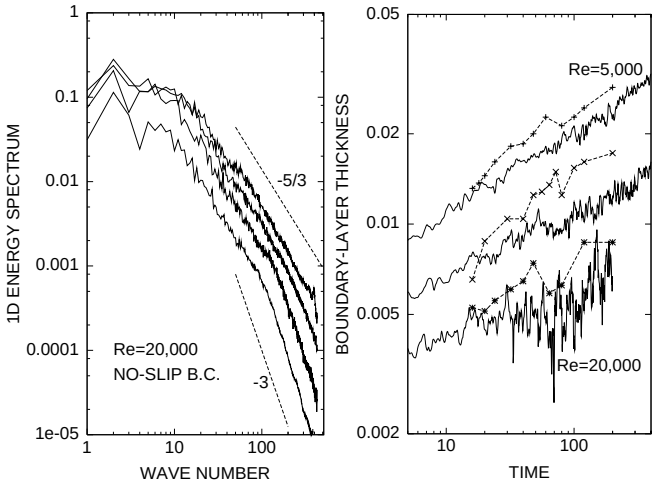

(a) (b)

FIG. 4. Time evolution of 1D spectra for runs with no-slip walls (Re = 20 000) (a) and the growth of $2\delta(\tau)$ (drawn lines) compared to the growth of $\lambda_i(\tau)$ ($- - + - -$ for Re = 5000, $- - \times - -$ for Re = 10 000, and $- - * - -$ for Re = 20 000) (b).

The authors gratefully acknowledge Dr. A. H. Nielsen for providing the Fourier pseudospectral code. One of us (H. J. H. C.) is grateful for support by the European Science Foundation (ESF-TAO/1998/13). This work was sponsored by the Stichting Nationale Computerfaciliteiten (National Computing Facilities Foundation, NCF) for the use of supercomputer facilities, with financial support from the Netherlands Organization for Scientific Research (NWO).

[1] R. H. Kraichnan, Phys. Fluids **10**, 1417 (1967).
[2] G. K. Batchelor, Phys. Fluids Suppl. II **12**, 233 (1969).
[3] U. Frisch and P. L. Sulem, Phys. Fluids **27**, 1921 (1984).
[4] P. Santangelo, R. Benzi, and B. Legras, Phys. Fluids A **1**, 1027 (1989).
[5] M. E. Brachet, M. Meneguzzi, and P. L. Sulem, Phys. Rev. Lett. **57**, 683 (1986).
[6] R. Benzi, S. Patarnello, and P. Santangelo, Europhys. Lett. **3**, 811 (1987).
[7] B. Legras, P. Santangelo, and R. Benzi, Europhys. Lett. **5**, 37 (1988).
[8] V. Borue, Phys. Rev. Lett. **72**, 1475 (1994).
[9] J. Sommeria, J. Fluid Mech. **170**, 139 (1986).
[10] J. Paret and P. Tabeling, Phys. Rev. Lett. **79**, 4162 (1997).
[11] H. Kellay, X-I. Wu, and W. I. Goldburg, Phys. Rev. Lett. **74**, 3975 (1995).
[12] M. A. Rutgers, Phys. Rev. Lett. **81**, 2244 (1998).
[13] H. J. H. Clercx, S. R. Maassen, and G. J. F. van Heijst, Phys. Rev. Lett. **80**, 5129 (1998).